

Real-time cardiac metabolism assessed with hyperpolarized [1-¹³C]acetate in a large-animal model

Alessandra Flori^a, Matteo Liserani^b, Francesca Frijia^c, Giulio Giovannetti^{c,d}, Vincenzo Lionetti^a, Valentina Casieri^a, Vincenzo Positano^c, Giovanni Donato Aquaro^c, Fabio A. Recchia^{a,e}, Maria Filomena Santarelli^{c,d}, Luigi Landini^{c,f}, Jan Henrik Ardenkjaer-Larsen^{g,h} and Luca Menichetti^{c,d,*}



Dissolution-dynamic nuclear polarization (dissolution-DNP) for magnetic resonance (MR) spectroscopic imaging has recently emerged as a novel technique for noninvasive studies of the metabolic fate of biomolecules *in vivo*. Since acetate is the most abundant extra- and intracellular short-chain fatty acid, we focused on [1-¹³C]acetate as a promising candidate for a chemical probe to study the myocardial metabolism of a beating heart. The dissolution-DNP procedure of Na[1-¹³C]acetate for *in vivo* cardiac applications with a 3 T MR scanner was optimized in pigs during bolus injection of doses of up to 3 mmol. The Na[1-¹³C]acetate formulation was characterized by a liquid-state polarization of 14.2% and a $T_{1\text{eff}}$ *in vivo* of 17.6 ± 1.7 s. *In vivo* Na[1-¹³C]acetate kinetics displayed a bimodal shape: [1-¹³C]acetyl carnitine (AcC) was detected in a slice covering the cardiac volume, and the signal of ¹³C-acetate and ¹³C-AcC was modeled using the total area under the curve (AUC) for kinetic analysis. A good correlation was found between the ratio AUC(AcC)/AUC(acetate) and the apparent kinetic constant of metabolic conversion, from [1-¹³C]acetate to [1-¹³C]AcC (k_{AcC}), divided by the AcC longitudinal relaxation rate (r_1). Our study proved the feasibility and the limitations of administration of large doses of hyperpolarized [1-¹³C]acetate to study the myocardial conversion of [1-¹³C]acetate in [1-¹³C]acetyl-carnitine generated by acetyltransferase in healthy pigs. Copyright © 2014 John Wiley & Sons, Ltd. Additional supporting information may be found in the online version of this article at the publisher's web site.

Keywords: hyperpolarization; dynamic nuclear polarization (DNP); magnetic resonance spectroscopy (MRS); free fatty acid (FA) metabolism; trityl radical; [1-¹³C]acetyl-carnitine; [1-¹³C]acetate; heart metabolism

1. INTRODUCTION

The dissolution-dynamic nuclear polarization (dissolution-DNP) technique (1) of specific metabolic substrates has been increasingly exploited for several metabolic studies *in vivo* by magnetic resonance spectroscopy (MRS) (2–4). The clinical relevance of its use was recently suggested in the first US Food and Drug Administration Investigational New Drug Study of Hyperpolarized Carbon-13 Metabolic MRI (5,6).

To date, [1-¹³C]pyruvate represents the reference molecule for hyperpolarized ¹³C magnetic resonance spectroscopic imaging (MRSI) (2,3) owing to its specific properties for dissolution-DNP experiments and its pivotal role in cell metabolism. In particular, the DNP formulation of [1-¹³C]pyruvic acid provides high ¹³C density, a long T_1 relaxation time and excellent self-glassing properties (2,7).

In addition to C-1- and C-2-labeled pyruvate (2,8–11), several ¹³C-enriched metabolic precursors were studied with dissolution-DNP technique (2,12–14). Acetate, a short chain fatty acid (SCFA), was suggested as a novel hyperpolarized substrate for use in DNP-enhanced MRSI, to define the pathways of SCFA cardiac metabolism in real time. In fact, fatty acids (FA) are the main myocardial energy substrate (15,16) of normal heart.

Acetate is taken up by cardiomyocytes and readily forms acetyl coenzyme-A (CoA), which is then transported into mitochondria after conjugation with carnitine by the enzyme carnitine acetyl-

* Correspondence to: L. Menichetti, Institute of Clinical Physiology, Via Moruzzi 1, I-56124, Pisa, Italy. Email: luca.menichetti@ifc.cnr.it

a A. Flori, V. Lionetti, V. Casieri, F. A. Recchia
Institute of Life Sciences, Scuola Superiore Sant'Anna, Pisa, Italy

b M. Liserani
Department of Physics, University of Pisa, Pisa, Italy

c F. Frijia, G. Giovannetti, V. Positano, G. D. Aquaro, M. F. Santarelli, L. Landini, L. Menichetti
Fondazione CNR/Regione Toscana G. Monasterio, Pisa, Italy

d G. Giovannetti, M. F. Santarelli, L. Menichetti
Institute of Clinical Physiology, National Council of Research, Pisa, Italy

e F. A. Recchia
Department of Physiology, Temple University School of Medicine, Philadelphia, PA, USA

f L. Landini
Department of Information Engineering, University of Pisa, Pisa, Italy

g J. H. Ardenkjaer-Larsen
GE Healthcare, Broendby, Denmark

h J. H. Ardenkjaer-Larsen
Department of Electrical Engineering, Technical University of Denmark, Kongens Lyngby, Denmark

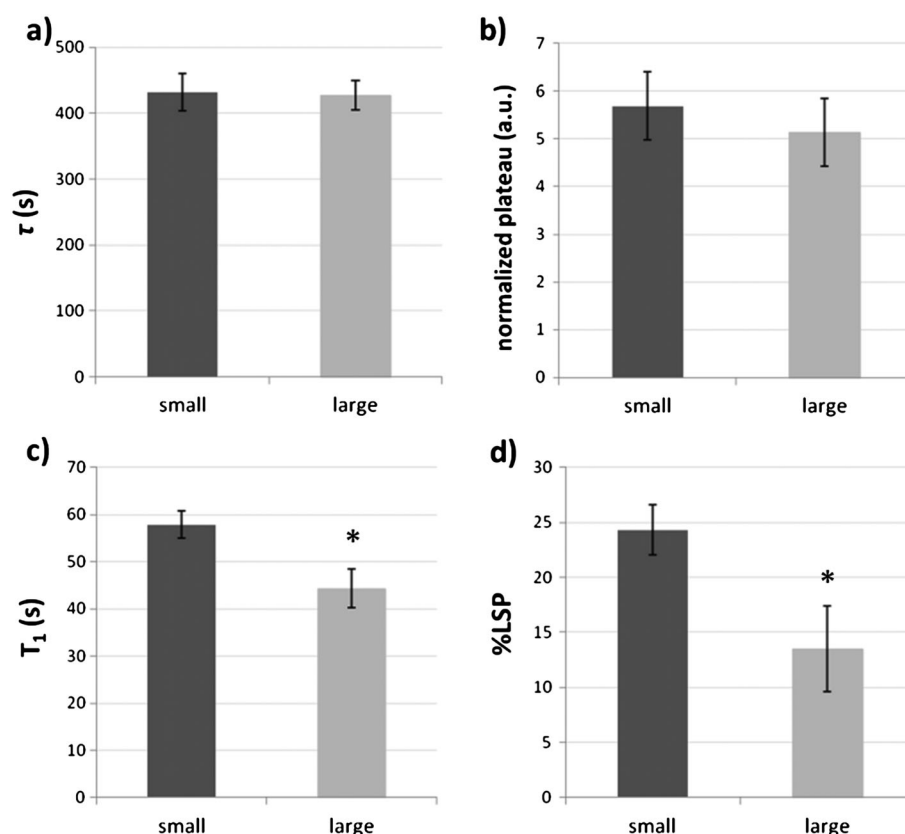


Figure 1. (a) Solid-state build-up time constants (τ); (b) normalized plateau values (\bar{I}); (c) T_1 relaxation time; (d) liquid state polarization percentage (%LSP), obtained for the hyperpolarized Na[1-¹³C]acetate small and large volumes (mean \pm SD). T_1 values were estimated at 1.05 T/40 °C from a mono-exponential fitting of the decay curve of the hyperpolarized signal (29).

transferase (10,17), and finally oxidized in the tricarboxylic acid (TCA) cycle. Fatty acid and glucose metabolism are competitive processes for the fuel supply to the heart that depends on aerobic vs anaerobic microenvironment, expression of enzymes and transporters or substrate concentration (16). Hyperpolarized [1-¹³C]acetate could be used to exploit with an MR scanner the role of SCFA as a competitor of glucose- and lactate-derived pyruvate, in order to provide structure and function information on the heart related to myocardial metabolism under resting and stress conditions. As previously described, [1-¹¹C]acetate has been used as a positron emission tomography (PET) tracer of TCA cycle activity and its efficacy as a marker of myocardial oxidative capacity has been clinically proven with this technique (18). However, the efficacy of hyperpolarized [1-¹³C]acetate as an MRSI marker of cardiac substrate selection is still not well proven in a model of human heart.

Even if the dissolution-DNP of [1-¹³C]acetic acid should be the most straightforward approach for the hyperpolarization of acetate, it was not performed owing to the inadequate glassy properties of this molecule (19). Nevertheless, the dissolution-DNP of [1-¹³C]acetic acid could be efficiently carried out with proper neutralization and buffering.

To date, tris(hydroxymethyl)aminomethane (*Tris*) [1-¹³C]acetate and sodium (Na) [1-¹³C]acetate formulations have been proposed for dissolution-DNP applications (20–27), while experiments *in vivo* have been conducted only in small animals. We previously tested hyperpolarized *Tris* [1-¹³C]acetate for MRSI in pigs (28). In the present study, we focused on the optimization of Na[1-¹³C]acetate

dissolution-DNP formulation and the implementation of a protocol for the hyperpolarization of large volumes to be injected in healthy pigs during real-time cardiac MRS.

2. RESULTS AND DISCUSSION

2.1. Dissolution-DNP Measurements

MRS and imaging experiments with hyperpolarized tracers require a dose scale-up proportional to the model body weight in order to increase the sensitivity. This represented a challenge in our experimental setting since Na[1-¹³C]acetate displays a known tendency to crystallize in a dose-dependent manner. We obtained a maximum ¹³C concentration of 7.3 m for Na [1-¹³C]acetate that is suitable for studies in large animals. The stability of the compound was most likely favored by glycerol supplementation, which improved the glassing properties of the mixture.

A dose escalation was performed following the same protocol previously described by us (29). The DNP performance at solid state of either small or large doses was compared considering the build-up time constant (τ) and the normalized plateau value (\bar{I}). We did not measure the solid-state polarization percentage of the Na [1-¹³C]acetate formulation, owing to the critical assessment of the thermal polarization. However, a direct comparison of the polarization enhancement of the samples could be performed through the \bar{I} value, which was proportional to the maximum solid-state polarization achievable with dissolution-DNP. The τ constant was

representative of the polarization dynamics and in particular of the speed of the polarization.

As a reference, we estimated the solid-state polarization of the large dose of $[1-^{13}\text{C}]$ acetate from the one previously measured for $[1-^{13}\text{C}]$ pyruvate. We obtained a solid-state polarization of approximately 20% by taking into account the Π value and the different amount of ^{13}C in each sample.

In addition, the liquid-state polarization percentage (%LSP) and T_1 variations were studied by switching to a larger dose. The %LSP and T_1 decreased respectively from 24 ± 2 to $14.2 \pm 4.0\%$ and from 58 ± 3 to 44 ± 4 s from the small ($n = 6$) to the large dose ($n = 8$), as shown in Fig. 1.

As shown in Fig. 1(a and b), the solid-state values (τ and $\bar{\Pi}$) were comparable for the small and the large doses, while the resulting T_1 and %LSP were significantly different after dissolution (Figs. 1c and 1d). The dissolution was the most critical step moving from the small to the large dose, using the Hypersense dissolution-DNP system. Similar results were also obtained by our group in a previous study with hyperpolarized $[1-^{13}\text{C}]$ pyruvate (29). Two main factors could contribute to decreasing the liquid-state polarization for the large dose compared with the small dose: (a) the slower and more critical dissolution process; and (b) the paramagnetic-induced relaxation given by the higher OX063 final concentration (0.22 ± 0.05 mM for the small dose and 0.56 ± 0.09 mM for the large dose).

The latter issue was a consequence of the different scale-up performed at solid- and liquid-state switching to larger dose. In fact, a 10-fold increase in the sample volume (from 60 up to 600 μl) was carried out to perform the solid-state polarization, whereas the dissolution volume was increased only 4 times (from 5 to 21 ml). These approaches were performed owing to both the limited capacity of the heating circuit of the polarizer and the need to maintain the final ^{13}C concentration as high as possible for *in vivo* injection.

Hence, we investigated how the %LSP and T_1 were affected by different OX063 concentrations (Fig. 2). These measurements were performed at 1.05 T and 40 °C by dissolution-DNP of Na $[1-^{13}\text{C}]$ acetate samples with different ^{13}C enrichments (20, 50 and 100%): the dissolution volume was chosen according to each sample in order to maintain a constant ^{13}C final concentration. The effect produced by different amounts of trityl radical on the liquid-state T_1 (Fig. 2) was quantified resulting in an increased relaxation rate R_1 proportional to the OX063 concentration [estimated longitudinal relaxivity of OX063 on the C-1 of acetate = $9.4 \text{ M}^{-1} \text{ s}^{-1}$, Fig. 2a]. A relaxometry study at low fields reported a value of $4.24 \text{ M}^{-1} \text{ s}^{-1}$ at 0.5 T and 37 °C for 80 mM pyruvate solution (30,31); the different field strength and in particular the presence of Gd^{3+} -chelate in the solution could explain the higher value measured by us.

Moreover, the trend of %LSP, estimated for the same dataset, parallels with the trend detected for the liquid-state T_1 , showing a decreased %LSP with increasing OX063 concentration (Fig. 2b). The same dataset allowed evaluation of the solid-state hyperpolarization performance of Na $[1-^{13}\text{C}]$ acetate at different ^{13}C concentration (using different ^{13}C enrichment). Therefore, as a control, we compared the normalized solid-state polarization values ($\bar{\Pi}$) and we found that $\bar{\Pi}$ values were not significantly affected by ^{13}C concentration in the range 1.5–7.3 M ($p > 0.05$, p -values determined by two-tailed Student's t -test; $n = 4$). Our findings were consistent with previous data obtained by other groups with different formulations, that is, $[1-^{13}\text{C}]$ pyruvate–

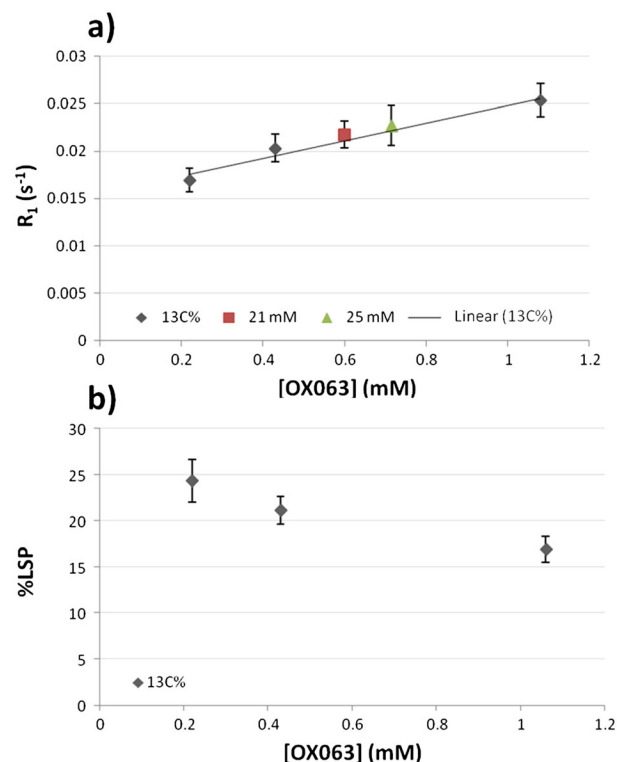


Figure 2. (a) The liquid-state relaxation rate (R_1) for the hyperpolarized Na $[1-^{13}\text{C}]$ acetate samples is reported with respect to the OX063 final concentration, after dissolution. The longitudinal relaxivity of OX063 on the C-1 of acetate was calculated from the linear fit of R_1 vs OX063 data ($R^2 = 0.97$). The samples at 21 and 25 mM OX063 were dissolved using the same dissolution volume (21 ml). (b) The %LSP for the hyperpolarized Na $[1-^{13}\text{C}]$ acetate samples is shown with respect to the OX063 final concentration, after dissolution. R_1 values were estimated at 1.05 T/40 °C from the hyperpolarized signal decay, as reported in Figure 1. 13C% indicates the data obtained after dissolution of Na $[1-^{13}\text{C}]$ acetate samples with different ^{13}C enrichment.

dimethyl-sulfoxide–OX063 and ^{13}C -acetate– H_2O :ethanol–TEMPO (7,22). According to these results, the observed %LSP variation was not correlated to previous differences at solid state.

For a separate dataset, we performed the dissolution-DNP of Na $[1-^{13}\text{C}]$ acetate samples with different OX063 concentrations (21 and 25 mM) using the same dissolution volume (21 ml). As shown in Fig. 2, the R_1 values obtained in this case were consistent with the linear fit previously reported. According to these data, it is conceivable that the paramagnetic-induced relaxation was the main factor leading to the reduction of the liquid-state polarization for the larger samples. Otherwise, the dissolution process (in terms of different volumes) had only a minor effect in our experimental setup.

A primary role of electron paramagnetic agents in the relaxation mechanism was also confirmed by NMR experiments performed for $[1-^{13}\text{C}]$ acetate at 9.4 T, where a significant reduction of the T_1 relaxation time was found for increasing OX063 concentrations. In particular, a value of $3.9 \text{ M}^{-1} \text{ s}^{-1}$ was found at 9.4 T and 25 °C for the C-1 relaxivity of 20%-enriched Na $[1-^{13}\text{C}]$ acetate samples at different OX063 final concentrations.

2.2. In vivo Experiments and MRS

Large animals are often the model of choice in translational medicine, since they better mimic aspects of human anatomy,

physiology and especially metabolism, compared with mice and rats (32). In particular, pigs are a well-known and well-characterized model of the human cardiovascular system.

The injection of hyperpolarized $[1-^{13}\text{C}]$ acetate in pigs required the preparation and optimization of a large dose in order to increase both the myocardial bioavailability of $[1-^{13}\text{C}]$ acetate and the maximum signal-to-noise ratio (SNR) during the MRS session. The dynamic conversion of $[1-^{13}\text{C}]$ acetate into its metabolite $[1-^{13}\text{C}]$ acetyl-carnitine ($[1-^{13}\text{C}]\text{AcC}$) was detectable in swine heart after the intravenous injection of 150 mmol of Na $[1-^{13}\text{C}]$ acetate.

The ^{13}C spectroscopic signals of Na $[1-^{13}\text{C}]$ acetate and of its metabolite $[1-^{13}\text{C}]\text{AcC}$ were detected using a 40 mm axial slice selected through the heart of the animal (Fig. 3a). The $[1-^{13}\text{C}]\text{AcC}$ peak was identified at -8.6 ppm (276 Hz) with respect to Na $[1-^{13}\text{C}]$ acetate in the ^{13}C spectrum (Fig. 3b, c).

The SNR is a critical aspect for hyperpolarized $[1-^{13}\text{C}]$ acetate in pigs. As shown in Fig. 3, the amplitude of the spectroscopic signal of $[1-^{13}\text{C}]\text{AcC}$ was typically 2 orders of magnitude lower than $[1-^{13}\text{C}]$ acetate (at the maximum value). The spectra at the maximum signals of $[1-^{13}\text{C}]$ acetate and $[1-^{13}\text{C}]\text{AcC}$ were selected and the SNR was estimated; a typical ratio of 1:25 was found for the AcC/acetate SNR. Low levels of $^{13}\text{C}\text{-AcC}$ were also reported by other groups in small animals (21,25), where the efficacy dose (mmol ^{13}C kg^{-1} body weight) was 1.5–5.5 times higher (0.123–0.44 mmol kg^{-1}) compared with the maximum value administered in this study (0.08 mmol kg^{-1}). Even if the rise of the injected dose could be beneficial to improve the SNR *in vivo*, the volume of the loading cap and the maximum achiev-

able ^{13}C concentration in this formulation limited the larger dose to a maximum of 3 mmol.

The use of different coil configurations, such as a transmit/receive circular coil (33) or a transmit-only birdcage and a receive-only circular coil (34), could improve the SNR of a maximum factor of 2 or 3 in the anterior left ventricular wall segments, which are closest to the circular coil (i.e. anterior and antero-lateral segments). However, the gain in sensitivity is still insufficient to allow a Chemical Shift Imaging (CSI) mapping of $^{13}\text{C}\text{-AcC}$.

The spectroscopic signal of $[1-^{13}\text{C}]$ acetyl CoA and of other metabolites (i.e. citrate) (27) could not be detected with this experimental approach owing to the very low abundance of the converted by-products and to insufficient spectroscopic resolution of 3 T scanner. A different strategy using a single 90° flip angle pulse was previously applied for the detection of $[1-^{13}\text{C}]$ acetyl CoA signal in small animals (21). The lack of $[1-^{13}\text{C}]$ acetyl CoA could also be attributed to the role of this molecule as an intermediate stage of the ^{13}C -acetate metabolic pathway (15,17). The metabolic curves, which describe the evolution over time of the spectroscopic signals of Na $[1-^{13}\text{C}]$ acetate and $[1-^{13}\text{C}]\text{AcC}$, were extracted (Fig. 4). The typical rise times recorded in the experiments ($n = 4$) were 9 ± 1 s for $[1-^{13}\text{C}]$ acetate and 24 ± 3 s for $[1-^{13}\text{C}]\text{AcC}$.

The dynamic data-set of $n = 4$ pigs was used to test the kinetics of the injected acetate. The evolution over time of the spectroscopic signal is determined by both the metabolic conversion and the magnetization loss owing to the hyperpolarization decay

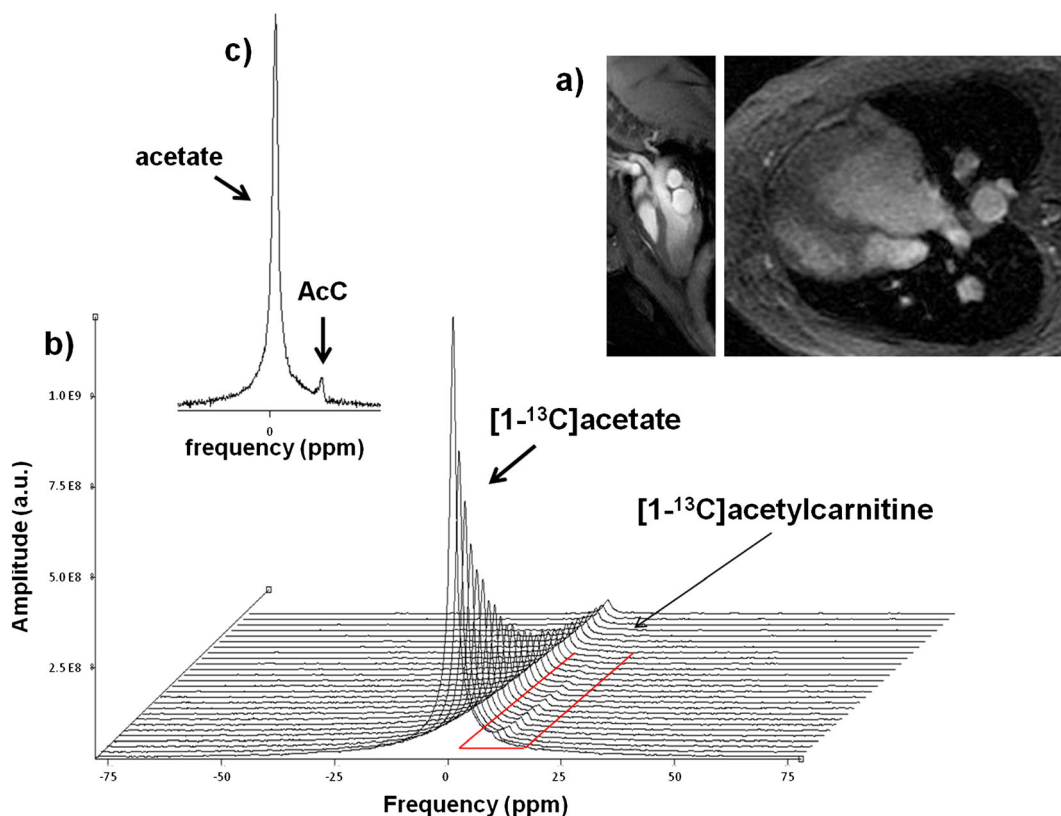


Figure 3. (a) Anatomical localization for MRS studies: a slice was selected through the heart of the pig (thickness = 40 mm); (b) dynamic evolution over time of $[1-^{13}\text{C}]$ acetate and $[1-^{13}\text{C}]\text{AcC}$ spectroscopic signals detected after bolus injection of hyperpolarized 150 mmol Na $[1-^{13}\text{C}]$ acetate; and (c) the spectra of $[1-^{13}\text{C}]$ acetate and $[1-^{13}\text{C}]\text{AcC}$ have been summed in the 20–36 s time interval.

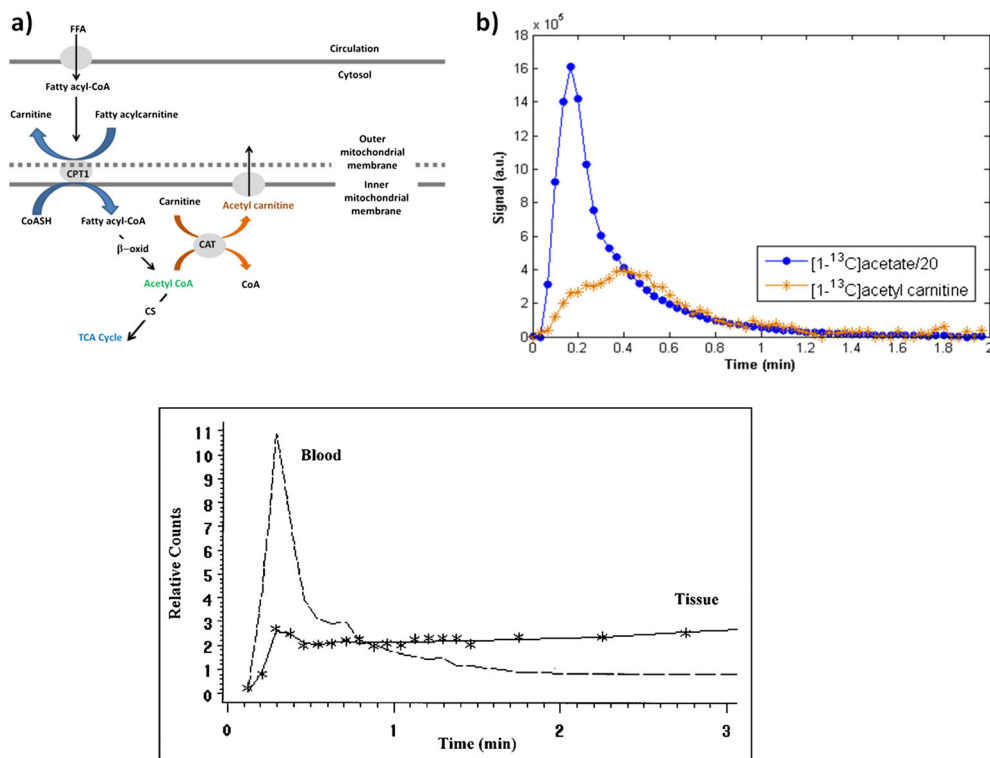


Figure 4. Panel 1: (a) graphic representation of the metabolic path of acetate in myocardial cells, where CAT stands for the enzyme carnitine acetyltransferase, CS stands for citrate synthase and CPT I is carnitine palmitoyltransferase I; FFA stands for free fatty acids, β -oxid for β oxidation and CoASH for the nonesterified form of CoA. (b) Typical dynamic metabolic curves of $[1-^{13}\text{C}]\text{acetate}$ and $[1-^{13}\text{C}]\text{AcC}$ obtained at 3 T from the spectroscopic signals after bolus injection of hyperpolarized 150 mM $\text{Na}[1-^{13}\text{C}]\text{acetate}$ in pigs. Panel 2: blood and myocardial ^{11}C -acetate tissue tracer activity data (symbols) along with model fits (solid line), from Sciacca *et al.* (36) by courtesy of the Editor.

and to RF excitations. We found a bimodal shape of the $[1-^{13}\text{C}]\text{acetate}$ signal as reported in Fig. 5, underlying a different behavior of acetate compared with similar cardiac studies with hyperpolarized $[1-^{13}\text{C}]\text{pyruvate}$ (11). In order to obtain the dynamic parameters *in vivo*, such as the effective T_1 ($T_{1\text{Eff}}$), the modeling of the $[1-^{13}\text{C}]\text{acetate}$ curve was performed using a γ -variate (11,35) [eqn (1)] and a mono-exponential fitting. The $[1-^{13}\text{C}]\text{acetate}$ $T_{1\text{Eff}}$ was estimated from the mono-exponential fitting of the final part of

the metabolic curve (Fig. 5): a value of $T_{1\text{Eff}} = 17.6 \pm 1.7$ s was found [corrected for the repetition time (TR) and flip angle]. The fitting parameters of the γ -variate function, describing the shape of the curve, are reported using box-plots in Fig. 5(b). The relative standard deviation (RSD) of the parameters was calculated in order to provide an index of statistical reliability of the estimates: the RSD was 9.7, 25 and 12.5% for the $T_{1\text{Eff}}$ and the γ -variate function parameters a and b , respectively.

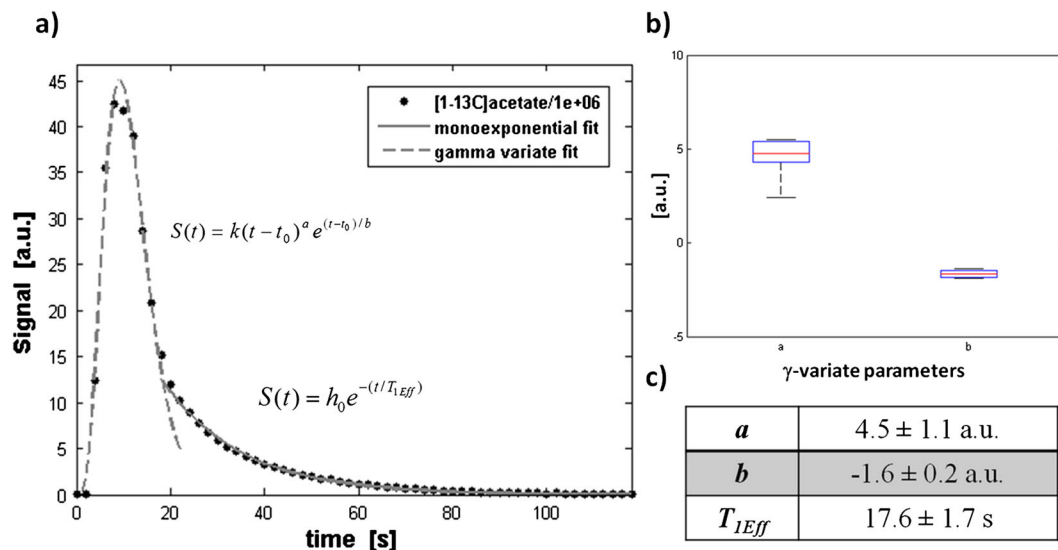


Figure 5. (a) Diagrammatic representation of the γ -variate and mono-exponential fitting of myocardial $[1-^{13}\text{C}]\text{acetate}$ metabolic curves; (b) box-plots of the fitting parameters a and b of the γ -variate function used to model the initial part of the $[1-^{13}\text{C}]\text{acetate}$ dynamic curve; and (c) values of the fitting parameters (mean \pm SD).

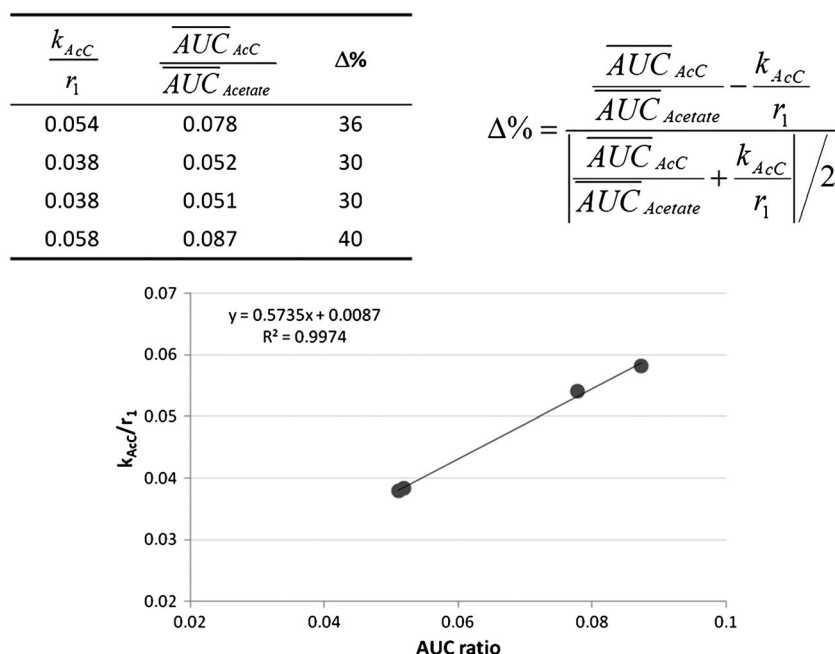


Figure 6. Correlation between the $AUC([1-^{13}C]AcC)/AUC([1-^{13}C]acetate)$ ratio and the apparent kinetic constant of metabolic conversion k_{AcC}/r_1 from $[1-^{13}C]acetate$ to $[1-^{13}C]AcC$, where r_1 is the $[1-^{13}C]AcC$ relaxation rate; the obtained values are reported in the Table (top left).

Taking into account the physiological variability of the animals, our results indicated a good inter-study reproducibility.

Positron emission tomography studies in humans were previously conducted using ^{11}C -acetate to evaluate oxygen consumption and myocardial perfusion (18,36–38). The typical time frame of these studies was of the order of 20–30 min, for which a bimodal shape of the time–activity curve of ^{11}C -acetate was found, underlying a compartmentalization of the tracer (18,37). However, in a few studies (36,38,39) early myocardial uptake of ^{11}C -acetate (60–180 s after i.v. injection) was also investigated (Fig. 4, panel 2) and a multicompartiment approach was proposed to analyze the kinetic uptake by myocardial tissue, using a two-compartment model to fit the first 3 min of the time–activity curve (36). In the present study, we investigated the same time-frame using a supra-physiological concentration of hyperpolarized ^{13}C -acetate [~ 3 –5 times more than the plasmatic concentration in pigs (40)]. Despite comparable dynamic profiles, we detected the metabolized fraction of acetate converted into $[1-^{13}C]AcC$ (Fig. 4).

According to similar findings reported using PET with ^{11}C -acetate (36,38,39), we suggest that the bi-phasic shape of the $[1-^{13}C]acetate$ curve was probably due to a compartmentalization of the tracer, where the first phase describes the bolus dynamics and the second phase describes a predominant contribution from myocardial uptake of $[1-^{13}C]acetate$.

In order to better investigate the $[1-^{13}C]acetate$ and the $[1-^{13}C]AcC$ kinetics, we applied a model based on the total area under the curve (AUC) (25,41) to the dynamic dataset (considering the second-phase of the acetate curve), which was compared with a standard two-site exchange model (11, see Additional Material).

A good correlation ($R^2 = 0.9974$, $n = 4$) was found between the ratio of the $AUC([1-^{13}C]AcC)/AUC([1-^{13}C]acetate)$ and the apparent kinetic constant of metabolic conversion from $[1-^{13}C]acetate$ into $[1-^{13}C]AcC$, divided by the $[1-^{13}C]AcC$ relaxation rate r_1 (Fig. 6). These results suggested that the spectroscopic signal of ^{13}C -acetate, detected in the second phase of the metabolic curve, mainly derives from intracellular acetate with a minor

contribution from the blood pool. To best of our knowledge, the slice-selective approach applied in our study did not allow the distinction between ^{13}C spectroscopic signals from the blood and myocardial tissue. This is a limitation for the full comprehension of the metabolic fate of hyperpolarized ^{13}C -acetate.

As a future perspective, the use of spectrally–spatially resolved acquisition sequences, able to detect the temporal evolution of the spectroscopic signal in the different regions of the heart, could clarify the *in vivo* ^{13}C -acetate kinetics, allowing the application of a multicompartimental model (42,43) or a semi-quantitative model-free approach based on the AUC.

Indeed, the analysis of $[1-^{13}C]acetate$ kinetics and $[1-^{13}C]AcC$ signal could provide insights into cardiac SCFA metabolism. The comparison of signals from hyperpolarized $[1-^{13}C]acetate$ and hyperpolarized $[1-^{13}C]pyruvate$ could represent a novel approach to investigating in real time the myocardial substrate selection *in vivo*.

Our protocol required the implementation of a few changes in the hardware configuration, namely caps to hold large doses and an upgraded design of the dissolution path to improve the dissolution of larger volumes. With regard to this, the recently developed ‘clinical’ polarizer (5) could certainly contribute to overcoming the hardware limitations, owing to the possibility to simultaneously polarize up to four sterile samples with increased volume ($>500 \mu l$).

3. CONCLUSIONS

We demonstrated that the real-time MRS assessment of cardiac metabolism is feasible in pigs using 3 T scanner and injectable dose up to $600 \mu l$ of $Na[1-^{13}C]acetate$ formulation. We found reproducible metabolic profiles displaying a bimodal pattern of the kinetic data. Our findings highlight a compartmentalization of the tracer, in accord with PET studies performed with ^{11}C -acetate. We obtained a semi-quantitative estimation of the acetate kinetic

of conversion into AcC using MRS and dissolution-DNP. The limitation of our study arises mainly from the kinetics of conversion and from the low SNR, given by the use of a volume coil and a limited amount of ^{13}C (~5–6 times lower in pigs) compared with small-animal studies. This is still a critical issue in performing CSI experiments in pigs. However, the reported results render $\text{Na}[1-^{13}\text{C}]\text{acetate}$ still a potential candidate for cardiac ^{13}C MRS with large-dose dissolution-DNP for diagnostic use.

4. EXPERIMENTAL

4.1. Sample Preparation for Dissolution DNP

$[1-^{13}\text{C}]\text{acetate}$ samples were prepared by dissolving $\text{Na}[1-^{13}\text{C}]\text{acetate}$ (Cambridge Isotope Laboratories Inc., Andover, MA, USA), trityl radical (OX063, Oxford Instr. Ltd, Abingdon, UK) and Gd^{3+} -chelate (Dotarem, Guebert, Roissy CdG Cedex, France) in a 60:40 w/w ultrapure (mQ, Millipore, Billerica, MA, USA) water–glycerol mixture. The mixture was sonicated at 60 °C until dissolution. The final concentration values were $\text{Na}[^{13}\text{C}\text{-acetate}] = 7.3 \text{ M}$, $[\text{OX063}] = 25 \text{ mM}$, $[\text{Gd}^{3+}\text{-chelate}] = 1.4 \text{ mM}$; $\text{Na}[1-^{13}\text{C}]\text{acetate}$ small doses (up to 60 μl) and large doses (up to 600 μl) were prepared as previously described and subsequently hyperpolarized. Samples with different ^{13}C isotopic enrichments (20, 50 and 100%, corresponding respectively to 1.5, 3.6 and 7.3 M ^{13}C concentration in the sample) and fixed OX063 concentration (25 mM) were also prepared. In a separate session of the study, samples with 7.3 M $\text{Na}[^{13}\text{C}\text{-acetate}]$ and different OX063 concentration (21 and 25 mM) were formulated.

4.2. Dissolution-DNP Measurements

DNP was performed using a commercial system (Hypersense[®], Oxford Instruments plc) slightly modified with an optimized design of the nozzle and using caps suitable for holding up to 800 μl , to allow the polarization and rapid dissolution of increased sample volumes. The samples were polarized at 3.35 T and 1.4 K for about 50 min. The maximum signal, normalized by the number of ^{13}C spins in the sample, ($\overline{\Pi}$) and the build-up time constants (τ), were estimated by fitting the build-up curves in Matlab (The Mathworks, Inc., Natick, MA, USA).

The dissolution of the hyperpolarized $\text{Na}[1-^{13}\text{C}]\text{acetate}$ samples was performed using different volumes of buffer (40 mM Trizma[®] pre-set crystals pH 7.6, Sigma-Aldrich, St Louis, MO, USA), 0.27 mM EDTA (ethylenediaminetetraacetic acid), Sigma-Aldrich and 50 mM NaCl, according to the sample amount. The final volumes were 5 ml for the small dose (up to 60 μl) and 21 ml for the large dose (up to 600 μl). In the latter case 10 ml was placed in the solvent container and 11 ml was added in the external receiving vessel, as described in our previous work (29). The final pH was 7.6 ± 0.2 and temperature was 37 ± 2 °C. The large dose was close to isotonic.

A 1 ml aliquot of the hyperpolarized solution was transferred to a 1.05 T NMR analyzer (Minispec MQ, Bruker BioSpin GmbH, Germany) for measurement of %LSP and T_1 , as described in the literature (29). The intensity of the hyperpolarized signal was measured at 40 °C, every 5 s for 200 s, using a 5° flip angle. The T_1 was obtained from the mono-exponential fit of the hyperpolarization decay curve, corrected for the flip angle and TR (44); the fitting was performed in Matlab.

Dissolution-DNP of the $\text{Na}[1-^{13}\text{C}]\text{acetate}$ samples with different ^{13}C enrichments was performed to study the %LSP and T_1 dependence on OX063 concentration ($n = 4$): a constant ^{13}C final

concentration was provided by selecting an appropriate dissolution volume for each sample. The relaxivity value was estimated at 1.05 T and 40 °C from the linear fit of the relaxation rate (R_1), measured at each OX063 concentration value. R_1 was calculated as T_1^{-1} , measured at 1.05 T and 40 °C as previously reported.

C-1 relaxivity was also determined at 9.4 T (VnmrS, Agilent Technologies, Santa Clara, CA, USA) for 20% enriched $\text{Na}[1-^{13}\text{C}]\text{acetate}$ samples with increased trityl radical concentration (0.44, 2.5 and 5 mM, respectively, ^{13}C -acetate final concentration ~90 mM) in a 40 mM Trizma[®] (Sigma-Aldrich), 0.27 mM EDTA (Sigma-Aldrich) buffer. T_1 was determined from a mono-exponential fit using an inversion recovery sequence; the longitudinal relaxivity was thus estimated at 9.4 T and 25 °C from the linear fit of the relaxation rate (R_1) as a function of the OX063 concentration. A Shigemi NMR tube was employed for the measurements at higher temperatures to minimize any convection effects.

4.3. Animal Protocol

We used four male healthy farm pigs (38–40 kg, b.w.). The animals were first sedated with a cocktail of tiletamine hydrochloride and zolazepam hydrochloride (8 mg kg⁻¹ i.m.) and pre-medicated with atropine sulfate (0.1 mg kg⁻¹) (11). A polyethylene catheter was inserted in the marginal ear vein for saline and drug infusion. Each experiment was performed after overnight fasting in lightly sedated animals with continuous infusion of propofol 1% (1 mg kg⁻¹ h⁻¹) at spontaneous breathing. A total of 600 μl of $\text{Na}[1-^{13}\text{C}]\text{acetate}$ sample was polarized and dissolved in 21 ml of buffer solution, using the same approach previously reported for the dissolution of large doses of $[1-^{13}\text{C}]\text{pyruvate}$ (29). The hyperpolarized $[1-^{13}\text{C}]\text{acetate}$ solution (150 mM acetate/20 ml $\approx 0.08 \text{ mmol kg}^{-1}$) was manually injected into the right ear vein over 10 s. Proton MRI and MRS were performed using a GE Excite HDX clinical 3 T scanner (GE Healthcare, USA) and a ^{13}C quadrature birdcage coil (Rapid Biomedical, Rimpf, Germany) while monitoring heart rate, rhythm and mean arterial pressure using an MR-compatible system (SA Instruments Inc., Stony Brook, NY, USA). The experimental protocol was approved by the Animal Care Committee of the Italian Ministry of Health and was in accordance with the Italian law (DL-116, Jan. 27, 1992), which is in compliance with the National Institutes of Health publication Guide for the Care and Use of Laboratory Animals.

The ^{13}C spectroscopic signals, detected in a 40 mm-thick axial slice placed over the heart of the animal, were acquired from the start of the injection, every 2 s for 120 s, using a (slice-selective) pulse-and-acquire sequence. A soft pulse excitation (bandwidth 2200 Hz, 2048 pts, 10° flip angle), with the center frequency adjusted to the acetate frequency, was employed for the acquisition. An anatomical reference image was acquired before the injection of the hyperpolarized compound using a cardiac-gated breath-hold single slice free precession sequence [field of view = 35 cm, flip angle = 45°, echo time (TE)/ TR = 1.71 ms/3.849 ms].

4.4. Post-processing

Peaks relative to $\text{Na}[1-^{13}\text{C}]\text{acetate}$ and $[1-^{13}\text{C}]\text{acetyl-carnitine}$ ($[1-^{13}\text{C}]\text{AcC}$) were identified using the AMARES algorithm as implemented in the jMRUI software package 3.0 (45). Initial conditions for the peak frequencies and line widths were provided by means of prior knowledge (Gaussian line shape, line

width = 0.0–20.0 Hz, [¹³C]acetate frequency = 0.0 Hz, [¹³C]AcC = 276 Hz).

Metabolic curves were produced by plotting the Na[¹³C]acetate and [¹³C]AcC signals as a function of time, in order to display the evolution over time of the signal of different metabolites. Fitting of the acetate curves was carried out in Matlab, using a mono-exponential and a γ -variate function, according to the following equation (35):

$$S(t) = k(t - t_0)^a e^{(t-t_0)/b} \quad (1)$$

where a , b , k are fitting parameters describing the shape of the curve and t_0 is the arrival time of the bolus and was set to 0 during the fitting process, assuming that the start of acquisition coincided with the arrival of the hyperpolarized compound at the region of interest in the myocardium. The fitting using the γ -variate was performed after correction for the $T_{1\text{eff}}$ decay, estimated from the mono-exponential fitting.

A two-site exchange model based on modified Bloch equations was used to fit the dynamic metabolic curves of [¹³C]acetate and [¹³C]AcC for the estimation of the apparent kinetic constant of metabolic conversion from [¹³C]acetate to [¹³C]AcC. An alternative method based on the total AUC of the [¹³C]acetate and [¹³C]AcC (41) was also applied and compared with the two-compartment model. The analysis was performed in Matlab; details of the two methods are reported in the Supporting Information.

Acknowledgements

We would like to thank Fondazione CNR/Regione Toscana 'G. Monasterio' (Pisa, Italy) for funding this study. We further thank Dr A. Dushpanova, Dr G. Bianchi and Mr F. Bernini for the helpful contribution for the animal model preparation, and Dr S. Bowen for NMR measurements. The project was also partially supported by the Italian FIRB funding RF-2010-2321788, and by NIH grants P01 HL-74237 and R01 HL108213.

REFERENCES

- Ardenkjaer-Larsen JH, Fridlund B, Gram A, Hansson G, Hansson L, Lerche MH, Servin R, Thaning M, Golman K. Increase in signal-to-noise ratio of >10,000 times in liquid-state NMR. *Proc Natl Acad Sci* 2003; 100(18): 10158–10163.
- Hurd RE, Yen Y-F, Chen A, Ardenkjaer-Larsen JH. Hyperpolarized ¹³C metabolic imaging using dissolution dynamic nuclear polarization. *J Magn Reson Imag* 2012; 36: 1314–1328.
- Gallagher FA, Kettunen MI, Brindle KM. Biomedical applications of hyperpolarized ¹³C magnetic resonance imaging. *Prog Nucl Magn Reson Spectrosc* 2009; 55: 285–295.
- Aime S, Dastrù W, Gobetto R, Santelia D, Viale A. Agents for polarization enhancement in MRI. *Handb Exp Pharmacol* 2008; 185 (I): 247–272.
- Ardenkjaer-Larsen JH, Leach AM, Clarke N, Urbahn J, Anderson D, Skoloss TW. Dynamic nuclear polarization polarizer for sterile use intent. *NMR Biomed* 2011; 24: 927–932.
- Nelson SJ, Kurhanewicz J, Vigneron DB, Larson P, Harzstarck A, Ferrone M, van Criekinge M, Chang J, Bok R, Park I, Reed G, Carvajal L, Small EJ, Munster P, Weinberg VK, Ardenkjaer-Larsen JH, Chen A, Hurd R, Odegardstuen L-I, Robb FJ, Tropp J, Murray JA. Metabolic imaging of patients with prostate cancer using hyperpolarized [¹³C] pyruvate. *Sci Transl Med* 2013; 5(198): 198ra108.
- Lumata L, Kovacs Z, Malloy C, Sherry AD, Merritt M. The effect of ¹³C enrichment in the glassing matrix on dynamic nuclear polarization of [¹³C]pyruvate. *Phys Med Biol* 2011; 56: N85–N92.
- Karlsson M, Jensen PR, Duus JØ, Meier S, Lerche MH. Development of dissolution DNP-MR substrates for metabolic research. *Appl Magn Reson* 2012; 43: 223–236.
- Schroeder MA, Lau AZ, Chen AP, Gu Y, Nagendran J, Barry J, Hu X, Dyck JRB, Tyler DJ, Clarke K, Connelly KA, Wright GA, Cunningham CH. Hyperpolarized ¹³C magnetic resonance reveals early- and late-onset changes to in vivo pyruvate metabolism in the failing heart. *Eur J Heart Fail* 2013; 15(2): 130–140.
- Schroeder MA, Atherton HJ, Dodd MS, Lee P, Cochlin LE, Radda GK, Clarke K, Tyler DJ. The Cycling of acetyl-CoA through acetylcarnitine buffer cardiac substrate supply: a hyperpolarized ¹³C magnetic resonance study. *Circul Cardiovasc Imag* 2012; 5(2): 201–209.
- Menichetti L, Frijia F, Flori A, Wiesinger F, Lionetti V, Giovannetti G, Aquaro GD, Recchia FA, Ardenkjaer-Larsen JH, Santarelli MF, Lombardi M. Assessment of real-time myocardial uptake and enzymatic conversion of hyperpolarized [¹³C]pyruvate in pigs using slice selective magnetic resonance spectroscopy. *Contrast Media Mol Imag* 2012; 7: 85–94.
- Mayer D, Yen Y-F, Josan S, Park JM, Pfefferbaum A, Hurd RH, Spielman DM. Application of hyperpolarized [¹³C]lactate for the in vivo investigation of cardiac metabolism. *NMR Biomed* 2012; 25: 1119–1124.
- Gallagher FA, Kettunen MI, Day SE, Hu D-E, Ardenkjaer-Larsen JH, in 't Zandt R, Jensen PR, Karlsson M, Golman K, Lerche MH, Brindle KM. Magnetic resonance imaging of pH in vivo using hyperpolarized ¹³C-labelled bicarbonate. *Nature* 2008; 453: 940–943.
- Bohndiek SE, Kettunen MI, Hu D-E, Kennedy BWC, Boren J, Gallagher FA, Brindle KM. Hyperpolarized [¹³C]-ascorbic and dehydroascorbic acid: vitamin C as a probe for imaging redox status in vivo. *J Am Chem Soc* 2011; 133: 11795–11801.
- Calvani M, Reda E, Arrigoni-Martelli E. Regulation by carnitine of myocardial fatty acid and carbohydrate metabolism under normal and pathological conditions. *Basic Res Cardiol* 2000; 95: 75–83.
- Stanley WC, Recchia FA, Lopaschuk GD. Myocardial substrate metabolism in the normal and failing heart. *Physiol Rev* 2005; 85:1093–1129.
- Fritz IB, Schultz SK, Srere PA. Properties of partially purified carnitine acetyltransferase. *J Biol Chem* 1963; 238: 2509–2517.
- Armbrecht JJ, Buxton DB, Brunken RC, Phelps ME, Schelbert HR. Regional myocardial oxygen consumption determined noninvasively in humans with [¹¹C]acetate and dynamic positron tomography. *Circulation* 1989; 80(4): 863–872.
- Bowen S, Ardenkjaer-Larsen JH. Formulation and utilization of choline based samples for dissolution dynamic nuclear polarization. *J Magn Reson* 2013; 236: 26–30.
- Jensen PR, Meier S, Ardenkjaer-Larsen JH, Duus JØ, Karlsson M, Lerche MH. Detection of low-populated reaction intermediates with hyperpolarized NMR. *Chem Commun* 2009; 34: 5168–5170.
- Jensen PR, Peitersen T, Karlsson M, in 't Zandt R, Gisselsson A, Hansson G, Meier S, Lerche MH. Tissue-specific short chain fatty acid metabolism and slow metabolic recovery after ischemia from hyperpolarized NMR in vivo. *J Biol Chem* 2009; 284(52): 36077–36082.
- Comment A, van den Brandt B, Uffmann K, Kurdzesau F, Jannin S, Konter JA, Hautle P, Wenckebach WTH, Gruetter R, van der Klink JJ. Design and performance of a DNP prepolarizer coupled to a rodent MRI scanner. *Conc Magn Reson B* 2007; 31B(4): 255–269.
- Comment A, Rentsch J, Kurdzesau F, Jannin S, Uffmann K, van Heeswijk RB, Hautle P, Konter JA, van den Brandt B, van der Klink JJ. Producing over 100 ml of highly concentrated hyperpolarized solution by means of dissolution DNP. *J Magn Reson* 2008; 194(1): 152–155.
- Mishkovsky M, Comment A, Gruetter R. In vivo detection of brain Krebs cycle intermediate by hyperpolarized magnetic resonance. *J Cereb Blood Flow Metab* 2012; 32: 2108–2113.
- Bastiaansen JA, Cheng T, Mishkovsky M, Duarte J MN, Comment A, Gruetter R. In vivo enzymatic activity of AcetylCoA synthetase in skeletal muscle revealed by ¹³C turnover from hyperpolarized [¹³C]acetate to [¹³C]acetylcarnitine. *Biochim Biophys Acta* 2013; 1830: 4171–4178.
- Kurdzesau F, van den Brandt B, Comment A, Hautle P, Jannin S, van der Klink JJ, Konter JA. Dynamic nuclear polarization of small labeled molecules in frozen water-alcohol solutions. *J Phys D Appl Phys* 2008; 41: 155506–155516.
- Bastiaansen JA, Cheng T, Gruetter R, Comment A. In vivo real time cardiac metabolism using hyperpolarized acetate. In *Proceedings of the 20th Annual Meeting ISMRM*, Melbourne, 2012.
- Menichetti L, Frijia F, Flori A, Lionetti V, Giovannetti G, Ardenkjaer-Larsen JH, Bianchi G, Romano SL, Liserani M, Aquaro GD, Positano V, Recchia FA,

- Landini L, Santarelli MF, Lombardi M. Hyperpolarized [^{13}C] acetate for cardiac 3D MRI metabolic imaging in middle size animal models. In Proceedings of the 5th Annual Meeting WMIC, Dublin, 2012; 008.
29. Flori A, Frijia F, Lionetti V, Ardenkjaer-Larsen JH, Positano V, Giovannetti G, Schulte R F, Wiesinger F, Recchia FA, Landini L, Santarelli MF, Lombardi M, Menichetti L. DNP methods for cardiac metabolic imaging with hyperpolarized [^{13}C]pyruvate large dose injection in Pigs. *Appl Magn Reson* 2012; 43: 299–310.
30. Chattergoon N, Martínez-Santesteban F, Handler WB, Ardenkjaer-Larsen JH, Scholl TJ. Field dependence of T_1 for hyperpolarized [^{13}C]pyruvate. *Contrast Media Mol Imag* 2013; 8: 57–62.
31. Miéville P, Jannin S, Bodenhausen G. Relaxometry of insensitive nuclei: Optimizing dissolution dynamic nuclear polarization. *J Magn Reson* 2011; 210: 137–140.
32. Dixon JA, Spinale FG. Large animal models of heart failure: a critical link in the translation of basic science to clinical practice. *Circul Heart Fail* 2009; 2(3): 262–271.
33. Giovannetti G, Hartwig V, Frijia F, Menichetti L, Positano V, Ardenkjaer-Larsen JH, Lionetti V, Aquaro GD, De Marchi D, Flori A, Landini L, Lombardi M, Santarelli MF. Hyperpolarized ^{13}C MRS cardiac metabolism studies in pigs: comparison between surface and volume radiofrequency coils. *Appl Magn Reson* 2012; 42: 413–428.
34. Giovannetti G, Frijia F, Hartwig V, Menichetti L, Positano V, Ardenkjaer-Larsen JH, Lionetti V, Aquaro G D, De Marchi D, Schulte RF, Wiesinger F, Landini L, Lombardi M, Santarelli MF. Transmit-only/receive-only radio-frequency system for hyperpolarized ^{13}C MRS cardiac metabolism studies in pigs. *Appl Magn Reson* 2013; 44: 1125–1138.
35. Blomley MJK, Dawson P. Bolus dynamics: theoretical and experimental aspects. *Br J Radiol* 1997; 70: 351–359.
36. Sciacca RR, Akinboboye O, Chou RL, Epstein S, Bergmann SR. Measurement of myocardial blood flow with PET using ^{11}C -acetate. *J Nucl Med* 2001; 42: 63–70.
37. van den Hoff J, Burchert W, Börner AR, Fricke H, Kühnel G, Meyer GJ, Otto D, Weckesser E, Wolpers HG, Knapp WH. [^{11}C]Acetate as a quantitative perfusion tracer in myocardial PET. *J Nucl Med* 2001; 42: 1174–1182.
38. Gropler RJ, Siegel BA, Geltman EM. Myocardial uptake of carbon-11-acetate as an indirect estimate of regional myocardial blood flow. *J Nucl Med* 1991; 32: 245–251.
39. Buck A, Wolpers HG, Hutchins GD, Savas V, Mangner TJ, Nguyen N, Schwaiger M. Effect of carbon-11-acetate recirculation on estimates of myocardial oxygen consumption by PET. *J Nucl Med* 1991; 32: 1950–1957.
40. Theil PK, Pedersen LJ, Jensen MB, Yde CC, Bach Knudsen KE. Blood sampling and hemolysis affect concentration of plasma metabolites. *J Anim Sci* 2012; 90: 412–414.
41. Hill DK, Orton MR, Mariotti E, Boulton JKR, Panek R, Jafar M, Parkes HG, Jamin Y, Falck Miniotis M, Al-Saffar MNS, Belouche-Babari M, Robinson SP, Leach MO, Chung Y-L, Eykyn TR. Modeling free approach to kinetic analysis of real-time hyperpolarized ^{13}C magnetic resonance spectroscopy data. *PLoS One* 2013; 8(9): e71996.
42. Zierhut ML, Yen Y-F, Chen AP, Bok R, Albers MJ, Zhang V, Tropp J, Park I, Vigneron DB, Kurhanewicz J, Hurd RE, Nelson SJ. Kinetic modeling of hyperpolarized $^{13}\text{C}_1$ -pyruvate metabolism in normal rats and TRAMP mice. *J Magn Reson* 2010; 202: 85–92.
43. Harrison C, Yang C, Jindal A, DeBerardinis RJ, Hooshyar MA, Merritt M, Dean Sherry A, Malloy CR. Comparison of kinetic models for analysis of pyruvate-to-lactate exchange by hyperpolarized ^{13}C NMR. *NMR Biomed* 2012; 25: 1286–1294.
44. Day IJ, Mitchell JC, Snowden MJ, Davis AL. Applications of DNP-NMR for the measurement of heteronuclear T_1 relaxation times. *J Magn Reson* 2007; 187: 216–224.
45. Vanhamme L, van den Boogaart A, Van Huffel S. Improved method for accurate and efficient quantification of MRS data with use of prior knowledge. *J Magn Res* 1997; 129: 35–43.

SUPPORTING INFORMATION

Additional supporting information may be found in the online version of this article at the publisher's web site.